Regulation of cold-induced thermogenesis by the RNA binding protein FAM195A

Jessica Cannavino[a,b,c], Mengle Shao[d,1], Yu A. An[d,1], Svetlana Bezprozvannaya[a,b,c], Shiuhwei Chen[d], Jiwoong Kim[e], Lin Xu[e], John R. McAnally[a,b,c], Philipp E. Scherer[d,f], Ning Liu[a,b,c], Rana K. Gupta[d], Rhonda Bassel-Duby[a,b,c], and Eric N. Olson[a,b,c,2]

[a]Department of Molecular Biology, University of Texas Southwestern Medical Center, Dallas, TX 75390; [b]Hamon Center for Regenerative Science and Medicine, University of Texas Southwestern Medical Center, Dallas, TX 75390; [c]Senator Paul D. Wellstone Muscular Dystrophy Specialized Research Center, University of Texas Southwestern Medical Center, Dallas, TX 75390; [d]Touchstone Diabetes Center, Department of Internal Medicine, University of Texas Southwestern Medical Center, Dallas, TX 75390; [e]Department of Population & Data Sciences, Quantitative Biomedical Research Center, University of Texas Southwestern Medical Center, Dallas, TX 75390; and [f]Department of Cell Biology, University of Texas Southwestern Medical Center, Dallas, TX 75390

Contributed by Eric N. Olson, April 29, 2021 (sent for review March 10, 2021; reviewed by Daniel P. Kelly and Peter Tontonoz)

Homeothermic vertebrates produce heat in cold environments through thermogenesis, in which brown adipose tissue (BAT) increases mitochondrial oxidation along with uncoupling of the electron transport chain and activation of uncoupling protein 1 (UCP1). Although the transcription factors regulating the expression of UCP1 and nutrient oxidation genes have been extensively studied, only a few other proteins essential for BAT function have been identified. We describe the discovery of FAM195A, a BAT-enriched RNA binding protein, which is required for cold-dependent thermogenesis in mice. FAM195A knockout (KO) mice display whitening of BAT and an inability to thermoregulate. In BAT of FAM195A KO mice, enzymes involved in branched-chain amino acid (BCAA) metabolism are down-regulated, impairing their response to cold. Knockdown of FAM195A in brown adipocytes in vitro also impairs expression of leucine oxidation enzymes, revealing FAM195A to be a regulator of BCAA metabolism and a potential target for metabolic disorders.

brown adipose tissue | thermogenesis | branched chain amino acids | RNA binding protein | disordered domain protein

Brown adipose tissue (BAT) has the unique ability to oxidize substrates and increase mitochondrial metabolism to produce heat through a process called nonshivering thermogenesis. The canonical pathway responsible for this form of heat production is based on the activity of mitochondrial uncoupling protein 1 (UCP1), which leads to the dissipation of chemical energy as heat (1, 2). Several transcriptional pathways are known to regulate UCP1 expression and thermogenic activation of brown adipocytes. Upon exposure to cold temperature, sympathetic nerves stimulate β-adrenergic receptors, which in turn, trigger the cyclic AMP-dependent protein kinase A (cAMP–PKA) pathway in brown adipocytes. Key transcription factors such as PR domain containing 16 (PRDM16), peroxisome proliferator-activated receptor-γ coactivator 1α (PGC1α), and peroxisome proliferation-activated receptor-γ (PPARγ) drive lipolysis along with an increase in the expression and activity of UCP1 and other mitochondrial genes (3, 4). The potential of BAT activation to counteract obesity and other metabolic disorders has generated great interest in the therapeutic potential of this process (5). Notably, the few RNA binding proteins (RBPs) that have been found to participate in BAT activation are ubiquitously expressed and have known functions in other tissues (6–11).

RBPs control key steps of RNA metabolism, from gene expression to protein translation, thereby playing critical roles in myriad cellular processes. Proteome-wide methodology, such as RNA interactome capture, has revealed a plethora of orphan RBPs with unknown functions (12). From a compendium of newly described putative RBPs, we identified FAM195A, a protein of unknown function with enriched expression in striated muscle. FAM195A and its homolog FAM195B were first identified as binding partners of the RNA helicase DDX6 in an in vitro tandem-protein pull-down screen in HEK293T cells (13). FAM195A is also annotated as mitogen-activated protein kinase (MAPK)-regulated corepressor interacting protein 2 (MCRIP2), following the reannotation of FAM195B as MCRIP1 due to its involvement in the MAPK pathway (14). However, no additional studies related to FAM195A protein expression or function have been reported.

Here, we show that FAM195A is a disordered domain protein localized to RNA stress granules, with enriched expression in striated muscle and BAT. FAM195A knockout (KO) mice have abnormal "whitening" of BAT and show fatal susceptibility to cold temperatures, indicating that FAM195A serves as an essential regulator of thermogenesis. Protein expression profiles in BAT of FAM195A KO mice compared to wild-type (WT) mice revealed aberrant branched-chain amino acid (BCAA) metabolism and fatty acid (FA) oxidation. Together, these findings reveal a previously undiscovered function of FAM195A as an essential regulator of body temperature during cold exposure, providing inroads into metabolic disease.

Results

FAM195A Is an RBP Enriched in Muscle and BAT. To identify and characterize putative RBPs highly expressed in striated muscle, we interrogated a list of previously uncharacterized putative

Significance

Activation of brown adipose tissue offers a strategy for enhancing energy expenditure to counteract obesity and other metabolic disorders. The discovery of novel factors regulating brown adipose tissue function has implications in therapeutic intervention to treat metabolic dysfunction. Here, we discover a previously uncharacterized RNA binding protein called FAM195A and show that genetically engineered mice lacking FAM195A are severely cold intolerant and have abnormalities in branched-chain amino acid metabolism. In vitro studies showed that FAM195A is required for the expression of enzymes involved in branched-chain amino acid catabolism. This study reveals FAM195A to be a link between thermoregulation, metabolism, and RNA processes, highlighting FAM195A as an important regulator of brown adipose tissue activation.

Author contributions: J.C., M.S., Y.A.A., R.K.G., and E.N.O. designed research; J.C., Y.A.A., S.B., S.C., J.K., L.X., and J.R.M. performed research; P.E.S. contributed new reagents/analytic tools; J.C., M.S., Y.A.A., R.K.G., N.L., R.B.-D., and E.N.O. analyzed data; and J.C., N.L., R.B.-D., and E.N.O. wrote the paper.

Reviewers: D.P.K., University of Pennsylvania Health System; and P.T., University of California Los Angeles.

The authors declare no competing interest.

[1]M.S. and Y.A.A. contributed equally to this work.

[2]To whom correspondence may be addressed. Email: eric.olson@utsouthwestern.edu.

This article contains supporting information online at https://www.pnas.org/lookup/suppl/doi:10.1073/pnas.2104650118/-/DCSupplemental.

Published June 4, 2021.

RBPs detected by the "mRNA interactome capture" technique. This approach identified over 1,000 RBPs in various cell types, many of which had no prior RNA-related annotation (12). Based on its enriched expression in striated muscle according to UCSC Genome Browser and no known function, we selected FAM195A as an RBP to further explore.

The mouse *Fam195a* gene is located on chromosome 17 and contains five exons that encode a protein of 160 amino acids with no identifiable domains other than a domain of unknown function (*SI Appendix*, Fig. S1*A*). This domain of unknown function, referred to as "FAM195," is present in FAM195A and FAM195B. The two proteins share 47% identity, with this homology being localized almost entirely to the FAM195 domain (*SI Appendix*, Fig. S1*B*). FAM195A also contains an extended disordered low-complexity domain, as is often found in RBPs that undergo phase separations (15) (*SI Appendix*, Fig. S1*C*). The FAM195A amino acid sequence is highly conserved throughout mammalian species, and protein orthologs have also been identified in zebrafish and *Xenopus* (*SI Appendix*, Fig. S1*D*).

In adult mouse tissues, qRT-PCR analysis revealed enrichment of the Fam195a transcript in all muscle groups analyzed, as well as in kidney and interscapular BAT (Fig. 1*A*). Western blot analysis of FAM195A expression using a commercial antibody against the full-length protein revealed strong expression in striated muscles and BAT (Fig. 1 *B* and *C*). Importantly, FAM195A protein expression was barely detected in inguinal white adipose tissue (iWAT) and epididymal white adipose tissue (eWAT) (Fig. 1*C*). Although FAM195A protein was detected in the liver and adrenal gland, the signal in the adrenal gland was likely due to the presence of BAT around the adrenal structure, as verified by expression of UCP1 in the same sample (Fig. 1*B*). Expression of Fam195a increases during in vitro adipogenic differentiation of cells from the stromal vascular fraction of brown adipose tissue (SVF-BAT), with an eightfold up-regulation of Fam195a transcript as early as 2 d after differentiation (*SI Appendix*, Fig. S2*A*).

FLAG-epitope–tagged FAM195A was found to colocalize with the RNA helicase DDX6 in RNA stress granules, upon inhibition of protein translation by sodium arsenite (13). To explore this further, we utilized a commercial antibody and obtained evidence of endogenous protein cellular localization, both with and without inhibition of protein translation. Western blot analysis of FAM195A in cytosolic and nuclear fractions of differentiated adipocytes revealed the protein to be localized in both compartments, albeit predominantly in the cytosolic fraction (Fig. 1*D*). Similarly, immunocytochemistry revealed a diffuse cytosolic and nuclear pattern of FAM195A in terminally differentiated adipocytes (Fig. 1*E*). In adipocytes treated with sodium arsenite to induce stress granule formation, FAM195A localized into distinct puncta in the cytosol, suggesting possible involvement of FAM195A with RNA processing pathways (Fig. 1*E*).

To determine if FAM195A is a bona fide RBP, we assessed the ability of an N-terminal TY1-FAM195A fusion protein to directly bind RNA in vitro using the polynucleotide kinase-mediated ^{32}P labeling of RNA after immunoprecipitation. SDS-PAGE of the eluted RNA resolved a strong signal starting at the expected molecular weight of TY1-FAM195A (Fig. 1*F*). The RNA smear corresponded to TY1–FAM195A–RNA complexes, as demonstrated by the absence of labeled RNA in samples either treated with high RNase concentration or obtained from cells that were not ultraviolet (UV) cross-linked (Fig. 1*F*). As a control for RNase digestion and cross-linking, protein–RNA complexes from each sample were immunoprecipitated using a primary antibody specific to heterogeneous ribonucleoprotein C (hnRNP/C), which showed similar results (Fig. 1*F*). These data demonstrate that FAM195A is an RBP that localizes to RNA stress granules in mature adipocytes.

Regulation of FAM195A Expression in BAT. Due to the restricted expression of FAM195A in BAT, we explored its involvement in metabolic models of browning of white adipose tissue (WAT) using the zinc finger protein 423 (Zfp423) KO mice, a mouse model in which iWAT undergoes browning (16). Indeed, we found that the Fam195a transcript was among the top 50 genes up-regulated in mice lacking Zfp423 in their adipose tissues (*SI Appendix*, Fig. S2*B*). These findings suggested that Fam195a is part of the gene expression program that is synchronously activated during the transition of WAT to a more mitochondria-enriched and thermogenic phenotype. In addition, by interrogating published ChIP-seq datasets (17, 18), we also found that the Fam195a promoter was bound by the transcriptional regulators Ebf2 and Pparg (*SI Appendix*, Fig. S2*C* and *Supplemental Methods*), which maintain the brown and/or beige fat cell identity. Finally, FAM195A protein was also regulated in differentiated stromal vascular fraction (SVF) cells derived from iWAT and treated with rosiglitazone, a drug known to stimulate mitochondrial biogenesis in vivo and in vitro (19) (*SI Appendix*, Fig. S2*D*).

FAM195A Loss of Function Causes BAT Whitening. To investigate the in vivo function of FAM195A, we generated a global FAM195A KO mouse line using the CRISPR-Cas9 system. By targeting exon 3 of the *Fam195a* gene, we obtained a founder line with a 93-base pair (bp) deletion, which removed 29 bp from the 3′ end of intron 2 and 64 bp from the 5′ end of exon 3 (*SI Appendix*, Fig. S3*A*). This deletion caused skipping of exon 3, as validated by sequencing of the BAT transcriptome in FAM195A heterozygous and KO animals (*SI Appendix*, Fig. S3*B*). The absence of exon 3 in the Fam195a transcript results in a premature stop codon and a predicted shorter version of the FAM195A protein that was not detected by western blot analysis in BAT from KO mice using a polyclonal antibody against the full-length protein (Fig. 2*F* and *SI Appendix*, Fig. S3 *C* and *D*).

FAM195A KO mice were born at Mendelian ratios from heterozygous intercrosses, and when maintained on normal chow, the fat and lean mass compositions, as measured by NMR, were not significantly different between WTs and KOs (Fig. 2*A*). Compared with WT animals, the KO mice did not show detectable differences in gross anatomy, tissue weight or histology of WAT, skeletal muscle, or heart tissues (Fig. 2*B* and *SI Appendix*, Fig. S3*F*). Hearts of KO animals displayed normal function, as assessed by echocardiography (*SI Appendix*, Fig. S3 *G* and *H*). However, BAT of animals lacking FAM195A was lighter in color and appeared hypertrophied as shown by an approximately twofold increase in tissue weight normalized to body weight (Fig. 2 *C*–*E*). Histologically, BAT from FAM195A KO mice contained abnormally large lipid droplets and resembled the morphology of WAT with large, unilocular adipocytes (Fig. 2 *D*, *Lower*). Despite significant whitening of BAT in FAM195A KO mice, the expression of UCP1 protein was unchanged (Fig. 2 *F* and *G*).

FAM195A Deficiency Causes Cold-Induced Hypothermia. Lipid accumulation in BAT is often associated with an abnormal physiological response to cold. To evaluate BAT thermogenesis in FAM195A KO animals, we performed an acute cold tolerance test. Mice were individually housed at 6 °C without food, bedding, or nesting materials, and their body temperatures were monitored for 5 h. FAM195A KO mice were significantly more cold sensitive than age-matched WT and heterozygous mice (Fig. 3*A* and Dataset S1). Furthermore, they became severely hypothermic with body temperatures <30 °C as early as 2 h after acute cold exposure (Fig. 3*B*). However, the shivering response in FAM195A KO animals was not affected, which suggests that FAM195A regulates thermogenesis independently of muscle activity (Fig. 3*C*). Moreover, KO animals performed similarly to WT animals both in single bouts of exhaustive running and in grip strength tests (*SI Appendix*, Fig. S3 *I*–*K*), further demonstrating that skeletal muscle function is not affected by the lack of FAM195A expression.

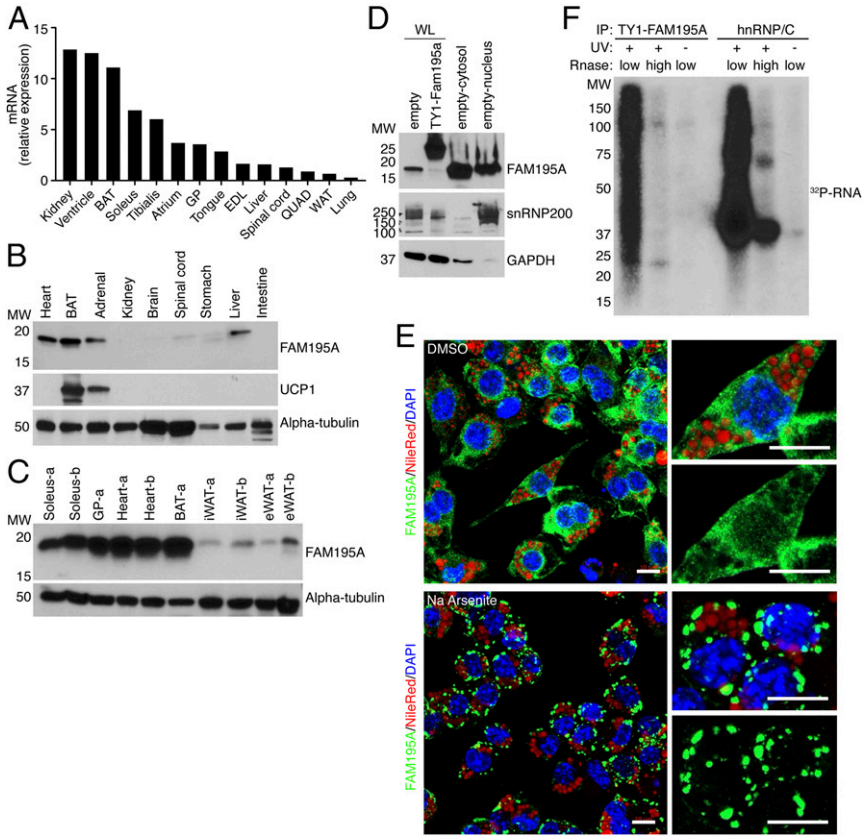

Fig. 1. FAM195A is enriched in muscle and BAT. (*A*) Detection of Fam195a mRNA by qRT-PCR in an adult mouse tissue library; 18S ribosomal RNA was used for normalization. Expression is shown relative to liver. (*B*) Detection of FAM195A and UCP1 proteins in adult mouse tissue homogenates by western blot analysis. The antibody against alpha-tubulin is used as the loading control. (*C*) Detection of FAM195A protein levels in different adipose tissue types and different muscle groups; alpha-tubulin protein was used as a loading control. The letters -a and -b represent lysates from two different animals. (*D*) Western blot analysis showing FAM195A protein in nuclear and cytosolic fractions obtained from differentiated adipocytes. snRNP200 and GAPDH protein are used as controls for cell fractionation efficiency. SVF cell lysate expressing TY1-FAM195A is the control for antibody specificity. (*E*) Immunofluorescence of FAM195A (green), DAPI for nuclei (blue), and Nile Red for lipid droplets (red). Staining was performed after 30′ incubation with sodium arsenite (500 μM) to induce stress granule formation or dimethyl sulfoxide (DMSO) as control. (Scale bars: 10 μm.) (*F*) Autoradiograph resolving the FAM195A–RNA complexes after immunoprecipitation (IP) of TY1-epitope–tagged FAM195A in UV cross-linked and uncross-linked adipocytes. As a control, UV cross-linked lysates were treated with high ribonuclease (RNase) concentration. hnRNP/C–RNA complexes were obtained as a control for RNA labeling and UV cross-linking. WL, whole cell lysate; MW, molecular weight; BAT, interscapular brown adipose tissue; EDL, extensor digitorum longus; GP, gastrocnemius plantaris; QUAD, quadricep; WAT, white adipose tissue.

Histological analysis of BAT after acute cold exposure revealed a low number of small lipid droplets in WT animals, whereas hyperlipidemia in FAM195A KO animals persisted (Fig. 3*D*). BAT sympathetic innervation is required for proper response to cold temperature. We did not observe significant differences in FAM195A KO BAT innervation compared with WT tissue, as shown by tyrosine hydroxylase immunoreactivity (20) (*SI Appendix*, Fig. S3 *L* and *M*).

qRT-PCR analysis of BAT from FAM195A KO mice maintained at room temperature showed that the expression of several thermogenesis-related genes was unchanged while UCP1 mRNA was down-regulated (Fig. 3*E*), despite the protein expression being unchanged (Fig. 2 *F* and *G*). Moreover, we assessed the expression of Prdm16, Pgc1α, Klf15, Esrra, and Ppara, all of which are responsible for metabolic adaptations (21–25). Among these genes, only Prdm16 mRNA was down-regulated (Fig. 3*F*). Finally, Pgc1α and Dio2 expression was equally induced by cold temperature in WT and KO animals, suggesting that other pathways essential for proper thermoregulation might be affected in FAM195A KO BAT (Fig. 3*E*).

Aberrant BCAA and FA Metabolism in BAT of FAM195A KO Animals. Stress granules consist primarily of RBPs, which are often directly or indirectly linked with protein translation (26). The localization of FAM195A within stress granules upon sodium arsenite treatment (Fig. 1*E*) suggested that FAM195A's function could be related to protein translation. To begin to explore this possibility, we performed proteomic analysis on isolated BAT from WT and KO animals. We identified 58 proteins that were down-regulated in FAM195A KO BAT by comparing proteins with expression of one $\log_2$ fold or greater in WT vs. KO (Fig. 4*A* and Dataset S2). High-confidence STRING (tool for the retrieval of Interacting Genes/Proteins) network analysis of the differentially expressed proteins resolved two clearly distinct clusters associated with FA oxidation, ketone body metabolism and mitochondria respiration (Fig. 4*B*). More detailed molecular function and biological process Gene Ontology (GO) analysis of affected proteins revealed that BCAA metabolism, FA β-oxidation, and oxidative phosphorylation (OXPHOS) complex I assembly were the top terms identified (*SI Appendix*, Fig. S4*A*). Similarly, the most represented GO term related to cellular component analysis was methylcrotonyl-CoA carboxylase complex, an enzymatic complex necessary for the catabolism of the BCAA leucine (*SI Appendix*, Fig. S4*A*). Notably, most of the enzymes involved in the BCAA leucine oxidation pathways were among the proteins down-regulated in FAM195A KO animals, with Isovaleryl-CoA dehydrogenase (IVD) being the most down-regulated protein in the dataset (*SI Appendix*, Fig. S4*F*). Branched-chain amino acid transaminase 2 (BCAT2), a key

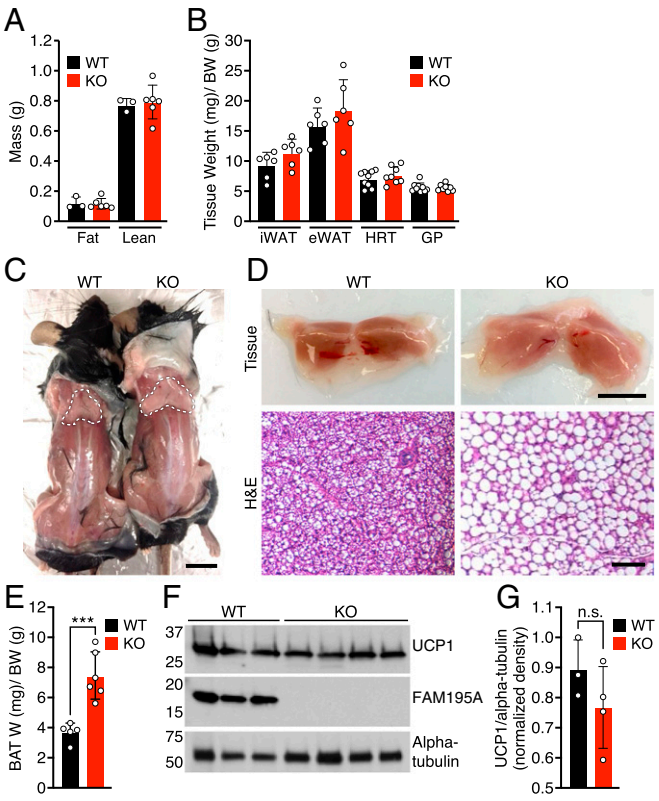

Fig. 2. FAM195A loss of function causes whitening of BAT tissues. (*A*) Body composition of mice measured by NMR (n = 3 WT; n = 6 KO). (*B*) Tissue weight of WT and FAM195A KO mice. Data are expressed as tissue weight normalized over body weight. iWAT and eWAT, n = 6 adult mice for each genotype; HRT and GP, n = 9 for WT and n = 8 for KO adult mice. (*C*) Representative photograph showing BAT of WT and FAM195A KO mice. The dotted white lines outline BAT tissues. (Scale bar: 1 cm.) (*D*) Morphology (*Upper*) and H&E staining (*Lower*) of WT and FAM195A KO BAT. (Scale bars: *Upper*, 500 mm; *Lower*, 50 μm.) (*E*) WT and FAM195A KO BAT weight. Data are expressed as BAT weight normalized to BW. n = 5 WT and n = 6 KO. ***$P < 0.001$. (*F*) Western blot analysis showing UCP1 and FAM195A protein expression in BAT from WT and FAM195A KO mice; alpha-tubulin was used as a loading control. (*G*) Quantification of western blot in *F*. Data are shown as mean ± SD; unpaired t test (*E*). W, weight; BW, body weight; iWAT, inguinal white adipose; eWAT, epididymal white adipose; HRT, heart; GP, gastrocnemius, plantaris; H&E, hematoxylin and eosin; n.s., not significant.

enzyme in BCAA metabolism, was also highly down-regulated (Fig. 4*A* and Dataset S2). Meanwhile, carnitine palmitoyltransferase 2 (CPT2), an enzyme essential to transporting FAs into mitochondria, was among the top 10 proteins identified as down-regulated in BAT from FAM195A KO mice. Interestingly, the expression of carnitine palmitoyltransferase 1b (CPT1B), the other mitochondria FA transporter, was unchanged both at the protein and at the RNA level (Fig. 4*C* and *SI Appendix*, Fig. S4*H*), suggesting that the lack of FAM195A expression did not result in a general alteration of BAT metabolism but rather, a more targeted effect.

Consistent with our findings, it has been previously reported that severe metabolic disorders result from mutations of either the *Bcat2* or *Cpt2* genes, highlighting their essential function for mitochondrial energy production and cell survival (27, 28). Strikingly, several down-regulated proteins in FAM195A KO BAT were found to be coexpressed with FAM195A by the unbiased GeneMANIA (multiple association network integration algorithm) database, demonstrating that FAM195A expression is regulated along with components of BCAA and mitochondria metabolism pathways (*SI Appendix*, Fig. S4*E*).

By performing RNA-sequencing (RNA-seq) analysis in different sets of WT and FAM195A KO animals, we found that 19 proteins identified in the proteomic experiments were also down-regulated at the transcriptional level. Interestingly, the common hits were predominantly related to leucine metabolism (*SI Appendix*, Fig. S4 *B*, *G*, and *H*). For all of the differentially expressed genes, BCAA and FA metabolism were among the most enriched GO terms (*SI Appendix*, Fig. S4 *C* and *D*). In addition, from both proteomic and transcriptomic analyses, we found several significantly enriched GO terms related to mitochondria RNA metabolism, such as mitochondria 5′- and 3′-end processing, mitochondria gene expression regulation, and mitochondria protein translation. (*SI Appendix*, Fig. S4 *A* and *C*).

To confirm the proteomic changes observed, we examined expression of CPT2 and branched-chain keto acid dehydrogenase E1 subunit-α (BCKDHA) by western blot analysis. We included BCKDHA in this analysis due to its recently reported involvement in nonshivering thermogenesis (29), along with being modestly down-regulated in our RNA-seq data. Western blot analysis confirmed a strong reduction of CPT2 and BCKDHA protein levels in FAM195A KO mice (Fig. 4*C*). In addition, we observed a marked reduction of OXPHOS complex I in all KO BAT lysates analyzed, validating the findings from the whole-tissue proteomic study (Fig. 4*C*). A significant decrease in OXPHOS complex I activity, as measured by the oxidation of NADH to NAD+ over time in FAM195A KO compared with control BAT lysates, was also seen (Fig. 4*D*). This confirms what was observed by western blot analysis of OXPHOS complexes (Fig. 4*C*).

It was previously shown that mice with BAT-specific deletion of BCKDHA displayed higher plasma BCAA levels than WT mice following cold exposure (29). This was found to be due to a failure to oxidize BCAAs in BAT, identifying this as a main site for BCAA clearance. Considering the fact that FAM195A KO animals present an overall down-regulation of BCAA metabolism, we sought to assess the BCAA content in these animals after 3 h of cold exposure. Leucine, valine, and isoleucine contents were each substantially increased in KO animals upon cold exposure, whereas the content of nonessential amino acids was unchanged or only slightly altered (Fig. 4*E* and Dataset S3). Taken together, our data suggest that oxidative metabolism is altered in FAM195A KO BAT with FA metabolism and BCAA clearance and oxidation being especially affected.

To elucidate whether these alterations could have an effect on BAT mitochondrial function and therefore, on the ability to thermoregulate, we measured oxygen consumption rates (OCRs) of FAM195A KO and heterozygous BAT tissue in the presence of individual BCAAs or the FA palmitate, both at baseline and with noradrenaline (NA) stimulation. Palmitate supplementation did not alter OCR in FAM195A KO BAT at baseline or after NA stimulation (Fig. 4*F*), indicating that FAs are properly oxidized in BAT lacking FAM195A. Similarly, OCR activity with both BCAA valine and isoleucine substrates did not show any significant difference in the FAM195A KO BAT compared with heterozygous tissues in either condition tested (Fig. 4*G*). However, the BCAA leucine substrate triggered significantly lower levels of mitochondrial OCR in FAM195A KO BAT at baseline. This difference, albeit at the limit of statistical significance, was maintained after NA stimulation (Fig. 4 *H* and *I*).

Knockdown of FAM195A In Vitro Is Sufficient to Alter the Expression of BCAA and CPT2 Enzymes. To determine the cell autonomous function of FAM195A, we infected BAT-derived SVF immortalized cells with different lentiviruses expressing short-hairpin RNAs (shRNAs) against Fam195a transcript or scrambled shRNA as a control. Upon differentiating the infected cells into adipocytes, we observed that shRNA-2 and shRNA-4 significantly decreased Fam195a transcript levels (~50 and ~70%, respectively), while sh-scramble and shRNA-5 did not have any effect (Fig. 5*A*).

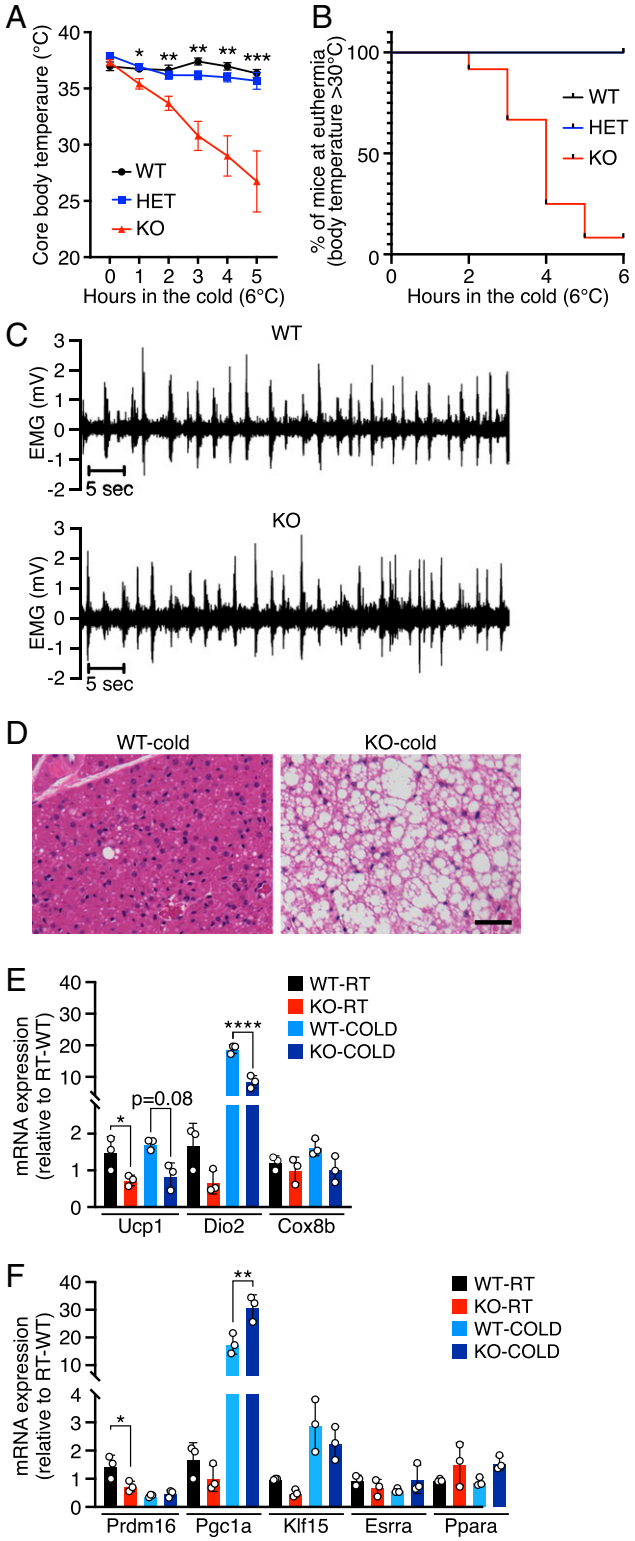

Fig. 3. Loss of function of FAM195A severely impairs thermogenesis. (*A*) Cold tolerance test at 6 °C of WT, HET, and FAM195A KO animals. $n = 3$ mice for the WT group, $n = 10$ mice for the HET group, and $n = 12$ mice for the KO group at T0. Animals were 12 wk old. $^{*}P < 0.05$; $^{**}P < 0.01$; $^{***}P < 0.001$. (*B*) Kaplan–Meier plots depicting mice maintaining euthermia (body temperature T > 30 °C) during the cold tolerance test in *A* for all genotypes. (*C*) Representative EMG measurements of muscle shivering in WT and FAM195A KO mice at 4 °C ($n = 4$ for each genotype). (*D*) H&E staining of WT and FAM195A KO BAT after cold tolerance test. (Scale bar: 50 μm.) (*E* and *F*) qRT-PCR analysis of thermogenic genes (*E*) and transcription factors (*F*) in WT and FAM195A KO BAT at room temperature and after cold tolerance test. Data are presented as mean ± SEM (*A*), mean ± SD (*E* and *F*), and one-way ANOVA (*A*, *E*, and *F*). RT, room temperature. $^{*}P < 0.05$; $^{**}P < 0.01$; $^{****}P < 0.0001$. WT, wild type; HET, heterozygous; KO, knock-out; T0, temperature before cold challenge; EMG, electromyography: H&E, hematoxylin and eosin.

Additionally, western blot analysis of shRNA scramble, shRNA-4, and shRNA-5 showed a clear reduction of FAM195A at the protein level (Fig. 5*B*). We observed no difference in the levels of differentiation of infected adipocytes as shown by Oil Red O staining (Fig. 5*C*). However, several components of the BCAA pathway identified as highly down-regulated in vivo by proteomics and RNA-seq analysis were also down-regulated in adipocytes infected with ShRNA-2 and ShRNA-4 but not in the cells infected with scramble and ShRNA-5 (Fig. 5*D*). Similar results were obtained when Cpt2 mRNA levels were tested, confirming the previous findings in vivo (*SI Appendix*, Fig. S4 *A*, *F*, and *G*). Interestingly, we did not observe significant down-regulation of Cox15 or Etfdh mRNA levels as observed in FAM195A KO BAT (Fig. 5*E*). Furthermore, CPT2 and BCKDHA protein levels were also markedly reduced upon FAM195A knockdown, demonstrating that the 50% down-regulation of their transcripts greatly impacts mitochondria protein expression and potentially, oxidative function (Fig. 5*F*). Therefore, these results point to the down-regulation of BCAA and FA enzymes observed in KO BATs as a direct effect of the lack of FAM195A expression.

FAM195A Interacts with Proteins Involved in Gene Expression and RNA Metabolism. To further investigate the molecular mechanism of FAM195A regulation of BAT thermogenesis in vivo, we performed a proximity labeling assay and obtained an unbiased list of proteins in close proximity to, and potentially interacting with, FAM195A. For these studies, the biotin ligase miniTurbo was fused to the C terminus of FAM195A and the plasmid transduced into SVF-BAT cells. Western blot analysis demonstrated stable and robust expression of FAM195A-miniTurbo–fused protein (Fig. 6*A*). SVF-BAT cells were differentiated into adipocytes and either pulsed for 2 h with 50 μM exogenous biotin (BIO+) or left untreated as a control (BIO−). Subsequently, proteomic analysis of streptavidin-purified biotinylated proteins was performed (Fig. 6*B*).

We next categorized the results of two independent experiments, listing those proteins with a ratio of abundance higher than 20 in BIO+ vs. BIO− immunoprecipitation in both datasets. By these criteria, the FAM195A interactome was found to be composed of 81 proteins (Fig. 6*C* and Dataset S4). Among the proteins recovered from BIO+ samples and undetected in the BIO− controls, we identified several regulators of splicing and maturation of mRNA such as FIP1L1, HNRNPA1, PRRC2A, SNW1, and SAFB (Fig. 6*C*). Accordingly, the GO analyses identified proteins related to RNA metabolism and RNA binding as among the top enriched terms (Fig. 6*D*). Finally, the RNA recognition motif was identified as the most significantly represented protein domain according to the simple modular architecture research tool (SMART) protein domain analysis (Fig. 6*E*). These findings place FAM195A protein among mRNA processing complexes, further corroborating FAM195A as a bona fide RBP.

Intriguingly, in addition to various RNA process GO terms, we also observed the presence of terms related to gene expression, DNA binding, and transcription by RNA polymerase II (Fig. 6*D*). Strikingly, proteins classified by these terms were also highly abundant and uniquely purified in BIO+ samples. Among these proteins, we identified well-known regulators of gene expression such as JUNB, TCF12, TCF20, ZNF281, NCOR1, and MED26.

To validate the proteins biotinylated by FAM195A, we performed another proximity ligation experiment wherein, prior to differentiation into mature adipocytes, cells were coinfected with FAM195A-miniTurbo and the N-terminal FLAG-HA–tagged

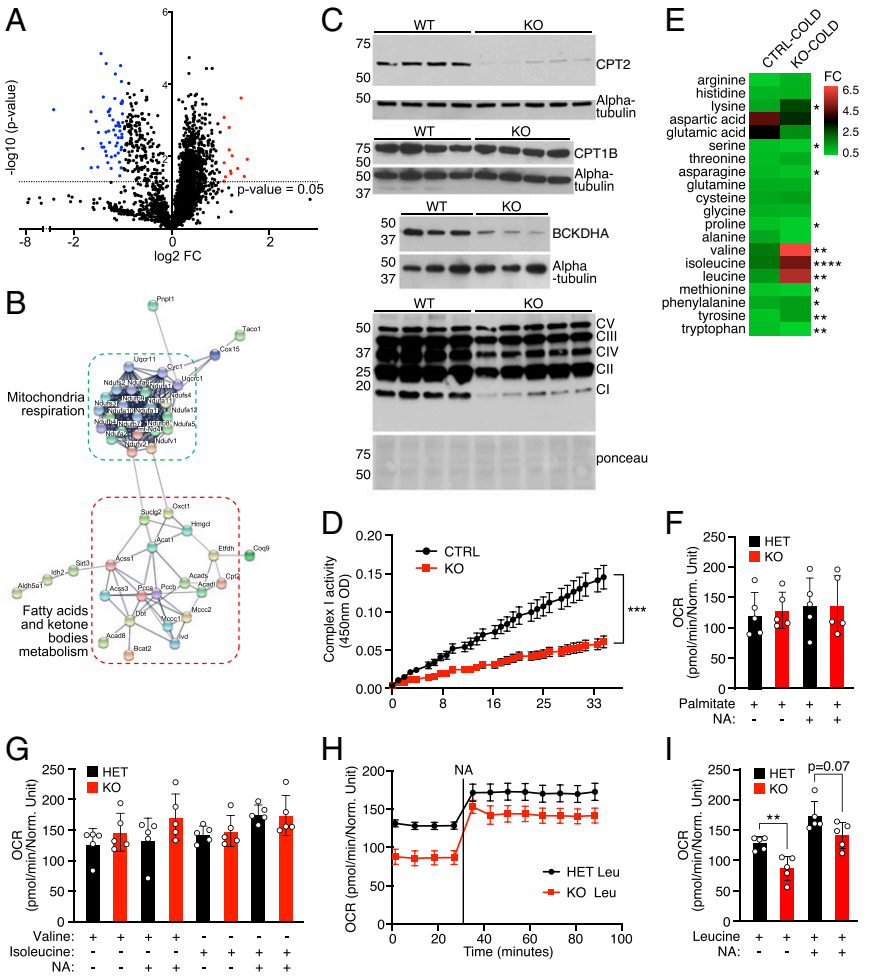

Fig. 4. Alterations in BCAA and FA metabolism in FAM195A KO BAT. (*A*) Volcano plot representing $\log_2$ (fold change [FC]) of proteins regulated in BAT FAM195A KO mice. $n = 3$ animals for each genotype. (*B*) STRING cluster analysis of proteins significantly down-regulated in *A*. (*C*) Western blot analysis showing BCKDHA, CPT2, CPT1B, and OXPHOS complexes expression in BAT homogenates from WT and FAM195A KO mice; alpha-tubulin and Ponceau red stain were used as loading controls. (*D*) Complex I activity measured in FAM195A KO and control (CTRL) lysates. $n = 5$ for CTRL (2 WT and 3 HET); $n = 6$ for KO. (*E*) Heat map showing FC of BCAA and amino acid content in plasma from CTRL and FAM195A KO animals after cold exposure. FCs were calculated by comparing the content of each BCAA and amino acid after cold exposure with the content in plasma collected at room temperature. $n = 4$ for CTRL (2 WT and 2 HET); $n = 4$ for KO. $^{*}P < 0.05$; $^{**}P < 0.01$; $^{****}P < 0.0001$. (*F*) OCR measurements of FAM195A KO and HET BAT in the presence of palmitate and NA stimulation. $n = 5$ for each genotype. (*G*) OCR measurements of FAM195A KO and HET BAT in the presence of valine and isoleucine before NA stimulation (time point 20 min) and after NA stimulation (time point 90 min). $n = 5$ for each genotype. (*H*) OCR measurements of FAM195A KO and HET BAT in the presence of leucine and NA. $n = 5$ for each genotype. (*I*) OCR measurements of FAM195A KO and HET BAT in the presence of leucine before NA stimulation (time point 20 min) and after NA stimulation (time point 90 min). $n = 5$ for each genotype. Data are presented as mean ± SEM (*D*, *H*) mean ± SD (*F*, *G*, and *I*); unpaired *t* test (*A*, *E*, *D*, and *I*). $^{**}P$ value < 0.01, $^{***}P < 0.001$. WT, wild-type; HET, heterozygous; KO, knock-out; CI-CV, OXOPHOS complexes I-V; O.D, optical density; OCR, oxygen consumption rate.

version of FIP1L1, SAFB, JUNB, and ZNF281. For each analyzed protein, we observed a positive FLAG signal by western blot analysis of the molecular weight of the correct protein only in the samples pulsed with biotin (Fig. 6 *F* and *G*). These results independently validate the proteomic analysis and locate FAM195A protein in close proximity with regulators of gene expression and mRNA processes.

FAM195A was reported to be a binding partner of DDX6 in vitro (13). Despite this, we did not detect significant enrichment of DDX6 in either of our experiments. However, we did identify DDX24, another member of the RNA helicase family, as one of the significantly enriched proteins. Finally, proteins participating in translation complexes were isolated, with EIF4B being identified as abundant in both experiments (Fig. 6*C*).

Discussion

Metabolic syndromes constitute a worldwide health problem due to their association with severe and life-threatening complications, including hypertension, peripheral vascular disease, and heart conditions (30). The browning of WAT is associated with an overall improvement of metabolism (31). Thus, the discovery of novel regulatory proteins participating in BAT activation could reveal new therapeutic targets for metabolic dysfunction. By examining an annotated collection of previously identified putative RBPs, we discovered a previously uncharacterized protein called FAM195A. Here, we show that FAM195A is an RBP that interacts with protein complexes participating in mRNA processing. Remarkably, mice lacking FAM195A are severely cold intolerant and present abnormalities in BCAA metabolism, highlighting FAM195A as a link between thermoregulation, metabolism, and RNA processes.

BCAA Metabolism in the Maintenance and Regulation of BAT Function. Brown adipocytes activate glucose, FA, and amino acid uptake during cold exposure (1). From the oxidation of these nutrients, the mitochondrial OXPHOS complexes create a proton gradient in the inner mitochondrial membrane, which is then dissipated in

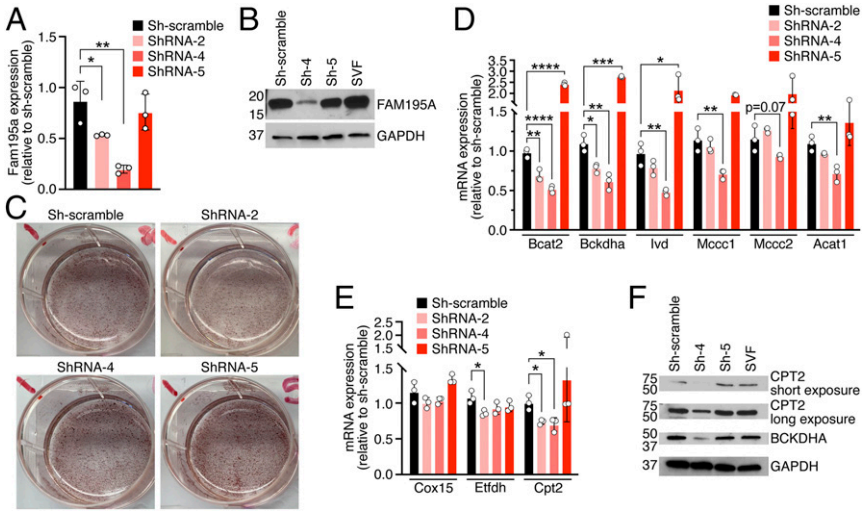

Fig. 5. Effects of FAM195A knockdown. (*A*) qRT-PCR analysis showing Fam195a mRNA expression in differentiated adipocytes expressing shRNAs scramble and shRNAs against Fam195a transcripts (ShRNA-2, ShRNA-4, and ShRNA-5). $*P < 0.05$; $**P < 0.01$. (*B*) Western blot analysis showing FAM195A protein levels in differentiated adipocytes expressing shRNAs scramble and shRNAs against Fam195a transcripts. GAPDH was used as a loading control. (*C*) Oil Red O staining of differentiated adipocytes expressing shRNA scrambled as a control and shRNAs against Fam195a transcripts. (*D* and *E*) qRT-PCR of selected genes related to BCAA metabolism (*D*) and mitochondria respiration (Cox15 and Etfdh) and FA transport (Cpt2; *E*) in differentiated adipocytes expressing shRNAs scramble and shRNAs against Fam195a transcripts. $*P < 0.05$; $**P < 0.01$; $***P < 0.001$ and $****P < 0.0001$. (*F*) Western blot analysis showing CPT2 and BCKDHA protein levels in differentiated adipocytes expressing shRNAs scramble and shRNAs against Fam195a transcripts. GAPDH was used as a loading control. Data are represented as mean ± SD (*A*, *D*, and *E*); unpaired *t* test (*A*, *D*, and *E*). SVF, stromal vascular fraction.

the form of heat by UCP1 proteins (1). By performing GO analysis of the whole-tissue proteome of FAM195A KO BAT, we observed the down-regulation of proteins involved in BCAA metabolism. Numerous proteins responsible for BCAA enzymatic reactions were significantly decreased, while all enzymes involved in leucine oxidation were strikingly underrepresented. This altered expression documents an aberrant utilization of the BCAA leucine in FAM195A KO animals. This idea is supported by the fact that mitochondrial basal respiration rate was decreased in FAM195A KO BAT compared to BAT from heterozygous mice when leucine was supplemented.

BCAA metabolism has been known for decades to have a direct effect on obesity (32, 33), and yet, its role in BAT physiology has only been recently explored. After a few hours of cold exposure, BCAA content in blood decreases, while enzymes involved in the first steps of BCAA oxidation, such as BCAT2 and BCKDHA, are selectively up-regulated (34). Subsequently, BCAAs begin to be utilized as a primary fuel for oxidative phosphorylation in both mice and humans (34). In separate studies, the loss of function of either the BCKDHA enzyme or the SLC25A44 amino acid transport channel in brown adipocytes impaired the response to cold with increased BCAA concentration in plasma compared with WT. These findings provide further evidence that BCAA oxidation is required for BAT thermogenesis (29).

We found that BCAT2, BCKDHA, and all proteins involved in leucine metabolism were among the numerous proteins down-regulated in the absence of FAM195A protein. Moreover, there was a striking up-regulation of all three BCAAs in the plasma of FAM195A KO animals after 3 h of cold exposure, demonstrating that these animals were unable to efficiently oxidize BCAAs in the cold. We postulate that FAM195A KO mice, like BCKDHA and SLC25A44 KO models, cannot utilize BCAAs, predominantly leucine, as fuel for optimal mitochondria oxidative phosphorylation and therefore, fail to survive in cold temperatures.

FA metabolism also plays an essential role in thermogenesis, due to FAs released by lipolysis serving as both an important nutrient fuel for oxidative phosphorylation and as allosteric activators of UCP1 protein during cold exposure (2). In FAM195A KO BAT, numerous enzymes involved in FA oxidation, such as CPT2, ACADS, ETFDH, and ACSL1, were down-regulated, with CPT2 being one of the most down-regulated proteins in FAM195A KO BAT. Mitochondria from animals lacking CPT2 protein are unable to utilize free FAs and therefore, become severely hypothermic after exposure to acute cold (35). Accordingly, the down-regulation of CPT2 and other FA metabolic enzymes in FAM195A KO animals suggests that, in addition to impaired BCAA metabolism, these animals are also unable to utilize free FAs. Despite no observed differences in the basal respiration rate when palmitate was supplemented to FAM195A BAT ex vivo, we cannot completely rule out the possibility that insufficient oxidation of FA might play a role in in vivo thermoregulation of FAM195A KO animals.

FAM195A Is an RBP That Functions as a Potential Regulator of Oxidative Metabolism. Our understanding of posttranslational regulation of RNA expression in BAT is still limited, with only a small number of RBPs, such as YBX2, IGFBP2, and HuR, having been identified as essential for adipogenesis and thermoregulation. Here, we demonstrate that FAM195A robustly binds RNA in adipocytes. RBPs are often found to be associated with various complexes and to regulate RNA at different steps of its processing. As an RBP, FAM195A may affect multiple RNA processes given its abundant cytosolic localization and its interaction with both the splicing factor Fip1L1 and the scaffold protein Safb, the latter of which forms molecular assembly points to couple DNA transcription with RNA maturation (36).

FAM195A is highly expressed in both BAT and striated muscles, each being tissues with high mitochondria content and high BCAA and FA oxidation rates (37). In addition, publicly available datasets (Gene Expression Omnibus [GEO] accession nos. 34204543 and 76221043) have indicated that FAM195A is up-regulated either in vitro upon PGC1α overexpression or following pharmacological treatment with rosiglitazone, both of which enhance mitochondria biogenesis. We found that FAM195A is up-regulated along with other canonical thermogenic genes in the absence of ZFP243, a protein necessary to maintain WAT metabolic identity in vivo (16). Moreover, according to available ChIP-seq data obtained from independent studies, Fam195a is transcriptionally regulated

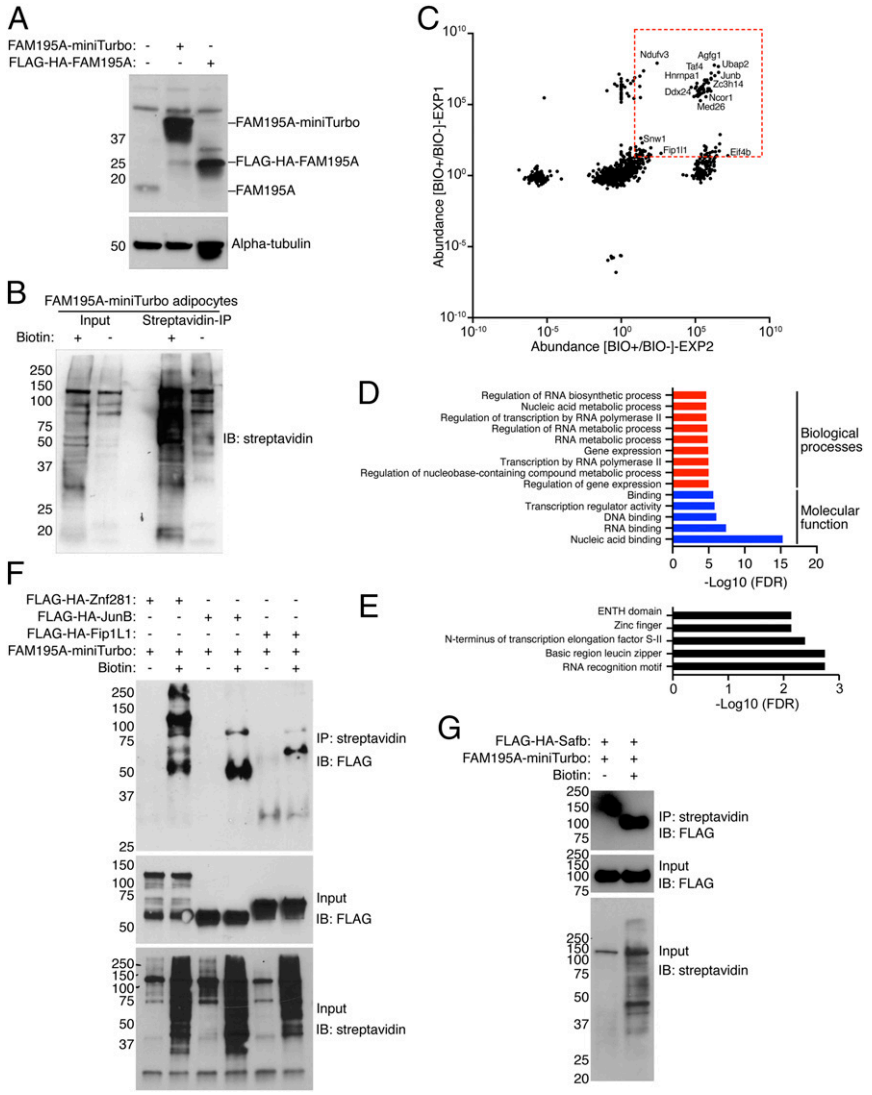

Fig. 6. FAM195A interactome in adipocytes. (*A*) Western blot analysis showing FAM195A-miniTurbo expression in differentiated adipocytes. FLAG-HA--FAM195A fusion protein was used as a control for antibody specificity; alpha-tubulin was used as loading control. (*B*) Western blot analysis showing protein biotinylation in the input lysate and precipitation of biotinylated proteins after streptavidin immunoprecipitation. (*C*) Volcano plot representing the abundance of proteins immunoprecipitated after proximity labeling in two independent experiments performed in differentiated adipocytes. The red dotted square contains protein with normalized abundance >20. (*D*) GO analysis of top enriched terms observed from *C*. (*E*) SMART protein domain analysis from *C*. (*F*) Western blot analysis of differentiated adipocytes coinfected with FAM195A-miniTurbo and FLAG-HA-Znf281, FLAG-HA-Junb, and FLAG-HA-Fip1L1. (*G*) Western blot analysis of differentiated adipocytes coinfected with FAM195A-miniTurbo and FLAG-HA-Safb. BIO+ cells were pulsed with biotin for 2 h, and BIO− cells were left untreated. IP, immunoprecipitation; IB, immunoblot.

by EBF2, PPARG, and PGC1α (17, 38), all key transcription factors for BAT development and activation, suggesting that FAM195A is a component in the molecular signature of BAT.

By evaluating the unbiased database GeneMANIA for genes coexpressed with FAM195A in mice, we found genes encoding several proteins that participate in BCAA metabolism, FA metabolism and mitochondria respiration. Expression of many of these proteins was also reduced in FAM195A KO BAT at both the protein and the mRNA levels, such as IVD, DBT, ETFB, NDUFS2, and TMEM143. Ultimately, by knocking down FAM195A expression in vitro in mature adipocytes, we observed a significant down-regulation of the BCAA leucine metabolism pathway, as well as CPT2 expression. This evidence confirms our observations in vivo and supports a direct correlation between FAM195A levels and the expression of BCAA enzymes and mitochondria respiration processes. Owing to FAM195A's RNA binding function and its interaction with transcription and RNA processing complexes, we theorized that FAM195A's function could be directly linked to the stabilization of mRNAs coding for these nutrient oxidation pathways.

Our findings establish the importance of the newly discovered BAT-enriched FAM195A RBP in regulating the expression of BCAA and FA metabolism enzymes, which in turn, determine the proper physiological response to cold. Future studies are needed to further characterize the FAM195A KO phenotype and fully address possible roles of other tissues in regulating body temperature in these animals. Taken together, our findings uncover an unrecognized pathway for the regulation of mitochondrial metabolism. A deeper understanding of FAM195A function may offer therapeutical interventions to treat metabolic disorders.

Methods

A full description of experimental materials and methods is provided *SI Appendix, Supplemental Methods*.

Generation of FAM195A KO Mice and Animal Studies. Animal work described in this manuscript has been approved and conducted under the oversight of the University of Texas Southwestern Institutional Animal Care and Use Committee. FAM195A KO mice were generated using CRISPR-Cas9 technology. C57BL/6 mice were utilized in all animal experimental procedures performed in this study, such as acute cold challenge, electromyography, treadmill running, grip strength assay, and transthoracic echocardiography, are described in *SI Appendix, Supplemental Methods*. Animals age and gender are indicated in figure legends or *SI Appendix, Supplemental Methods*.

Cell Lines. The immortalized SVF cell line derived from BAT and iWAT of adult C57BL/6 animals was established as previously described (16). Differentiation into mature adipocytes was induced by treating confluent cultures with different media as described in *SI Appendix, Supplemental Methods*.

RNA Preparation for qRT-PCR and RNA Sequencing. After dissection, BAT tissues were snap frozen in liquid nitrogen and pulverized with mortar and pestle. For RT-PCR, RNA was prepared as follows. Total RNA was extracted from BAT using TRIzol (Ambion), and cDNA was synthetized using Super Script III (Invitrogen), according to the provider's protocol. qRT-PCR was performed using the ABI ViiA7 PCR cycler. For RNA sequencing ($n = 3$ mice per genotype), RNA was extracted using the RNeasy Micro kit (74004; Qiagen) as per the provider's instructions. RNA-seq analysis was performed as described in *SI Appendix, Supplemental Methods*.

Western Blot Analysis and Whole-Tissue Proteomics. For western blot analysis and whole-tissue proteomics, protein lysates were extracted using radioimmunoprecipitation assay lysis buffer (R0278; Sigma) supplemented with protein inhibitors (Roche). Protein concentration was determined by bicinchoninic acid assay (23225; ThermoFisher), and equal amounts of protein among samples were used for regular western blot and transferred to polyvinylidene fluoride (PVDF) membrane (IPVH00010; Millipore). Immunodetection was performed using Western Blotting Luminol Reagent (sc2048; Santa Cruz Biotechnology) or Amersham ECL prime (RPN 2232; GE Healthcare). Whole-tissue proteomic analysis was performed as described in *SI Appendix, Supplemental Methods*.

Statistics. Data are presented as mean ± SD or mean ± SEM as indicated in each figure. Statistical analysis was performed as indicated in each figure.

Data Availability. The RNA-seq dataset has been deposited in the GEO repository (National Center for Biotechnology Information; accession no. GSE164964). The mass spectrometry dataset has been deposited in the MassIVE Repository (accession no. MSV000086711). All other data are included in the article and/or supporting information.

ACKNOWLEDGMENTS. We thank Jose Cabrera for graphics, John Shelton for help with histology, Laurent Gautron for providing probes and apparatus for electromyography experiments, Joshua Heinrich for assistance in performing running experiment, Alex Mireault for performing grip strength assay, Wei Tan for performing echocardiograms, and Kenian Chen for analysis of published ChIP-seq data. We also thank Kedryn Baskin and Christine Kusminski for helpful discussion. We thank the Genomics and Microarray Core for RNA-seq, the Histo Pathology Core for histological analysis and expertise, the University of Texas Southwestern Proteomics Core for mass spectrometry, and the University of Texas Southwestern Metabolic Phenotyping Core for the liquid chromatography with tandem mass spectrometry analysis of free amino acids in plasma samples. This work was supported by funds from NIH Grants HL130253, AR071980, and AR-067294; Senator Paul D. Wellstone Muscular Dystrophy Specialized Research Center Grant P50HD087351; Career Development Award 19CDA34670007 from American Heart Association and the Harry S. Moss Heart Trust (to M.S.); NIH, National Institute of Diabetes and Digestive and Kidney Diseases Grant K01-DK125447 (to Y.A.A.); NIH, National Institute of Diabetes and Digestive and Kidney Diseases Grants R01 DK104789 (to R.K.G.), R56 DK119163 (to R.K.G.), and R01 DK119163 (to R.K.G.); and Robert A. Welch Foundation Grant 1-0025 (to E.N.O.).

1. B. Cannon, J. Nedergaard, Nonshivering thermogenesis and its adequate measurement in metabolic studies. *J. Exp. Biol.* **214**, 242–253 (2011).
2. A. Fedorenko, P. V. Lishko, Y. Kirichok, Mechanism of fatty-acid-dependent UCP1 uncoupling in brown fat mitochondria. *Cell* **151**, 400–413 (2012).
3. T. C. Leone *et al.*, PGC-1alpha deficiency causes multi-system energy metabolic derangements: Muscle dysfunction, abnormal weight control and hepatic steatosis. *PLoS Biol.* **3**, e101 (2005).
4. P. Seale, Transcriptional control of brown adipocyte development and thermogenesis. *Int. J. Obes.* **34**, S17–S22 (2010).
5. Y. H. Tseng, A. M. Cypess, C. R. Kahn, Cellular bioenergetics as a target for obesity therapy. *Nat. Rev. Drug Discov.* **9**, 465–482 (2010).
6. J. Pihlajamäki *et al.*, Expression of the splicing factor gene SFRS10 is reduced in human obesity and contributes to enhanced lipogenesis. *Cell Metab.* **14**, 208–218 (2011).
7. M. E. Huot *et al.*, The Sam68 STAR RNA-binding protein regulates mTOR alternative splicing during adipogenesis. *Mol. Cell* **46**, 187–199 (2012).
8. C. F. Chou *et al.*, KSRP ablation enhances brown fat gene program in white adipose tissue through reduced miR-150 expression. *Diabetes* **63**, 2949–2961 (2014).
9. N. Dai *et al.*, IGF2BP2/IMP2-deficient mice resist obesity through enhanced translation of Ucp1 mRNA and other mRNAs encoding mitochondrial proteins. *Cell Metab.* **21**, 609–621 (2015).
10. J. Wang *et al.*, RNA-binding protein PSPC1 promotes the differentiation-dependent nuclear export of adipocyte RNAs. *J. Clin. Invest.* **127**, 987–1004 (2017).
11. D. Xu *et al.*, RNA binding protein Ybx2 regulates RNA stability during cold-induced brown fat activation. *Diabetes* **66**, 2987–3000 (2017).
12. A. Castello *et al.*, Insights into RNA biology from an atlas of mammalian mRNA-binding proteins. *Cell* **149**, 1393–1406 (2012).
13. R. Bish *et al.*, Comprehensive protein interactome analysis of a key RNA helicase: Detection of novel stress granule proteins. *Biomolecules* **5**, 1441–1466 (2015).
14. K. Ichikawa *et al.*, MCRIP1, an ERK substrate, mediates ERK-induced gene silencing during epithelial-mesenchymal transition by regulating the co-repressor CtBP. *Mol. Cell* **58**, 35–46 (2015).
15. B. A. Ozdilek *et al.*, Intrinsically disordered RGG/RG domains mediate degenerate specificity in RNA binding. *Nucleic Acids Res.* **45**, 7984–7996 (2017).
16. M. Shao *et al.*, Zfp423 maintains white adipocyte identity through suppression of the beige cell thermogenic gene program. *Cell Metab.* **23**, 1167–1184 (2016).
17. S. Rajakumari *et al.*, EBF2 determines and maintains brown adipocyte identity. *Cell Metab.* **17**, 562–574 (2013).
18. S. N. Shapira *et al.*, EBF2 transcriptionally regulates brown adipogenesis via the histone reader DPF3 and the BAF chromatin remodeling complex. *Genes Dev.* **31**, 660–673 (2017).
19. L. Wilson-Fritch *et al.*, Mitochondrial biogenesis and remodeling during adipogenesis and in response to the insulin sensitizer rosiglitazone. *Mol. Cell. Biol.* **23**, 1085–1094 (2003).
20. X. Zeng *et al.*, Innervation of thermogenic adipose tissue via a calsyntenin 3β-S100b axis. *Nature* **569**, 229–235 (2019).
21. L. Fan, P. N. Hsieh, D. R. Sweet, M. K. Jain, Krüppel-like factor 15: Regulator of BCAA metabolism and circadian protein rhythmicity. *Pharmacol. Res.* **130**, 123–126 (2018).
22. P. Lefebvre, G. Chinetti, J. C. Fruchart, B. Staels, Sorting out the roles of PPAR alpha in energy metabolism and vascular homeostasis. *J. Clin. Invest.* **116**, 571–580 (2006).
23. R. B. Vega, D. P. Kelly, A role for estrogen-related receptor alpha in the control of mitochondrial fatty acid beta-oxidation during brown adipocyte differentiation. *J. Biol. Chem.* **272**, 31693–31699 (1997).
24. J. A. Villena *et al.*, Orphan nuclear receptor estrogen-related receptor alpha is essential for adaptive thermogenesis. *Proc. Natl. Acad. Sci. U.S.A.* **104**, 1418–1423 (2007).
25. P. Xue *et al.*, BCKDK of BCAA catabolism cross-talking with the MAPK pathway promotes tumorigenesis of colorectal cancer. *EBioMedicine* **20**, 50–60 (2017).
26. S. Jain *et al.*, ATPase-modulated stress granules contain a diverse proteome and substructure. *Cell* **164**, 487–498 (2016).
27. X. L. Wang, C. J. Li, Y. Xing, Y. H. Yang, J. P. Jia, Hypervalinemia and hyperleucine-isoleucinemia caused by mutations in the branched-chain-amino-acid aminotransferase gene. *J. Inherit. Metab. Dis.* **38**, 855–861 (2015).
28. P. J. Isackson, M. J. Bennett, G. D. Vladutiu, Identification of 16 new disease-causing mutations in the CPT2 gene resulting in carnitine palmitoyltransferase II deficiency. *Mol. Genet. Metab.* **89**, 323–331 (2006).
29. T. Yoneshiro *et al.*, BCAA catabolism in brown fat controls energy homeostasis through SLC25A44. *Nature* **572**, 614–619 (2019).
30. K. B. Keller, L. Lemberg, Obesity and the metabolic syndrome. *Am. J. Crit. Care* **12**, 167–170 (2003).
31. A. Abdullahi, M. G. Jeschke, Taming the flames: Targeting white adipose tissue browning in hypermetabolic conditions. *Endocr. Rev.* **38**, 538–549 (2017).
32. L. A. Lotta *et al.*, Genetic predisposition to an impaired metabolism of the branched-chain amino acids and risk of type 2 diabetes: A Mendelian randomisation analysis. *PLoS Med.* **13**, e1002179 (2016).
33. C. B. Newgard *et al.*, A branched-chain amino acid-related metabolic signature that differentiates obese and lean humans and contributes to insulin resistance. *Cell Metab.* **9**, 311–326 (2009).
34. M. Chondronikola *et al.*, Brown adipose tissue activation is linked to distinct systemic effects on lipid metabolism in humans. *Cell Metab.* **23**, 1200–1206 (2016).
35. E. Gonzalez-Hurtado, J. Lee, J. Choi, M. J. Wolfgang, Fatty acid oxidation is required for active and quiescent brown adipose tissue maintenance and thermogenic programing. *Mol. Metab.* **7**, 45–56 (2018).
36. H. W. Liu, T. Banerjee, X. Guan, M. A. Freitas, J. D. Parvin, The chromatin scaffold protein SAFB1 localizes SUMO-1 to the promoters of ribosomal protein genes to facilitate transcription initiation and splicing. *Nucleic Acids Res.* **43**, 3605–3613 (2015).
37. M. D. Neinast *et al.*, Quantitative analysis of the whole-body metabolic fate of branched-chain amino acids. *Cell Metab.* **29**, 417–429.e4 (2019).
38. S. A. Ochsner *et al.*, The Signaling Pathways Project, an integrated 'omics knowledgebase for mammalian cellular signaling pathways. *Sci. Data* **6**, 252 (2019).